Cerebral Cortex October 2009;19:2466–2478
doi:10.1093/cercor/bhp002
Advance Access publication February 11, 2009

Attention Reshapes Center-Surround Receptive Field Structure in Macaque Cortical Area MT

Katharina Anton-Erxleben, Valeska M. Stephan and Stefan Treue

Cognitive Neuroscience Laboratory, German Primate Center, Kellnerweg 4, 37077 Göttingen, Germany

Directing spatial attention to a location inside the classical receptive field (cRF) of a neuron in macaque medial temporal area (MT) shifts the center of the cRF toward the attended location. Here we investigate the influence of spatial attention on the profile of the inhibitory surround present in many MT neurons. Two monkeys attended to the fixation point or to 1 of 2 random dot patterns (RDPs) placed inside or next to the cRF, whereas a third RDP (the probe) was briefly presented in quick succession across the cRF and surround. The probe presentation responses were used to compute a map of the excitatory receptive field and its inhibitory surround. Attention systematically reshapes the receptive field profile, independently shifting both center and surround toward the attended location. Furthermore, cRF size is changed as a function of relative distance to the attentional focus: attention inside the cRF shrinks it, whereas directing attention next to the cRF expands it. In addition, we find systematic changes in surround inhibition and cRF amplitude. This nonmultiplicative push–pull modulation of the receptive field's center-surround structure optimizes processing at and near the attentional focus to strengthen the representation of the attended stimulus while reducing influences from distractors.

Keywords: motion processing, physiology, spatial summation, tuning, visual system

Introduction

At any moment, we process only a small amount of the information captured by our sensors. Attention is the nervous system's main mechanism to enhance processing of relevant information at the cost of irrelevant information. In the visual system, paying attention to a particular location in space increases perceptual sensitivity, accuracy, and spatial resolution and speeds up reaction times near the attentional focus (e.g., Posner et al. 1980; Hawkins et al. 1990; Yeshurun and Carrasco 1998; Carrasco et al. 2002) while perceptually suppressing unattended stimuli (O'Regan et al. 1999).

Physiologically, attention strengthens the representation of attended aspects of the visual scene across visual cortex by modulating responses of those neurons that are involved in processing these aspects (see Treue 2003; Serences and Yantis 2006, for reviews). Spatial attention selectively modulates firing rates of neurons with receptive fields overlapping the attended region in visual space (e.g., Treue and Maunsell 1996, 1999; Reynolds et al. 2000; Williford and Maunsell 2004) and is also evident in a spatially selective modulation of blood oxygen level–dependent responses (Tootell et al. 1998; Brefczynski and DeYoe 1999).

Although earlier studies have suggested that attention increases not only the sensitivity but also the selectivity of individual neurons for features like stimulus orientation or motion direction (Haenny and Schiller 1988; Spitzer et al. 1988), more recent research has shown that attention modulates orientation and direction tuning curves in a multiplicative fashion without changing the tuning width (McAdams and Maunsell 1999; Treue and Martinez-Trujillo 1999; Martinez-Trujillo and Treue 2004). In the spatial domain, however, attentional effects can appear to be nonmultiplicative even on the single neuron level: recent experiments have found that receptive field profiles shift toward an attended location (V4: Connor et al. 1996, 1997; LIP [lateral parietal area]: Ben Hamed et al. 2002; MT [medial temporal area]: Womelsdorf et al. 2006) and receptive field area shrinks when attention is shifted into the receptive field (MT: Womelsdorf et al. 2006). Even though multiplicative modulations at preceding stages may underlie these changes, they are effectively nonmultiplicative in nature and do change the selectivity of individual neurons by shifting and sharpening their spatial tuning curves.

Receptive fields in many visual areas have a complex substructure and consist not only of an excitatory receptive field center (the classical receptive field [cRF]) but often have a surrounding region (the non-cRF), where stimuli are thought not to drive the cell by themselves but modulate responses to a central stimulus. We have studied attentional effects on receptive fields in the motion processing area MT, where antagonistic surrounds are common that act inhibitory when stimulated with the cell's preferred direction (Tanaka et al. 1986; Lui et al. 2007). The exact proportion of MT cells which have such a surround varies from 50% (Perge et al. 2005) to ~79% (Raiguel et al. 1995; Lui et al. 2007). Surrounds in area MT extend widely beyond the cRF radius by a factor ranging from 3–4 (Raiguel et al. 1995) to 7–10 (Allman et al. 1985; Tanaka et al. 1986) in different studies. Nearly half of MT surrounds seem to be spatially biased toward one side of the cRF rather than being arranged circularly around it (Xiao et al. 1995; but see Tanaka et al. 1986).

Attention might differentially change the influence of attended and unattended stimuli on the neuronal response, and accordingly on perception, by selectively modulating receptive field surrounds around the attentional focus. Such an attentional modulation of suppressive versus integrative effects of receptive field surrounds has recently been found in area V1 and is so far the only direct evidence for an attentional impact on non-cRF regions (Roberts et al. 2007; see also Ito and Gilbert 1999, for an indirect measure of attentional effects on surround facilitation in V1). Recent studies show that in area MT as well as in V1, surround influences are not fixed but modifiable by stimulus properties and perceptual context and may even switch from inhibition to facilitation (V1: Kapadia

et al. 1999; Sceniak et al. 1999; MT: Pack et al. 2005; Huang et al. 2007). However, whether *attention* modulates receptive field surrounds in extrastriate areas has not yet been tested.

For area MT, we recently showed that attentional modulation of *cRF* regions comprises not only a change in spatial summation but more prominently a shift of the receptive field profile (Womelsdorf et al. 2006). If attention does affect receptive field surrounds in area MT, the question remains therefore if attention would shift the surround profile in a similar fashion toward (or away) from the attentional focus rather than simply up- or down-modulating surround suppression. Such a spatially specific strengthening of center-surround antagonism near the attentional focus might be a mechanism by which attention selectively suppresses unattended stimuli that are close by.

Here, we study how inhibitory surrounds are modulated by spatial attention in area MT. Specifically, we test if inhibitory surrounds shift toward or away from an attended stimulus by mapping cRFs and non-cRFs under different attentional conditions with high resolution. Additionally, we provide new insights into attentional modulation of receptive field sizes and summation properties in area MT.

Materials and methods

Monkey Training and Surgery

Two male rhesus monkeys (*Macaca mulatta*) were trained to perform a visual spatial attention task. Following standard operant conditioning procedures, we used fluid reward as positive reinforcement for each correct trial in training and recording sessions. Animals were implanted with a custom made orthopedic implant to prevent head movements during training and recording, and a recording chamber (Crist Instruments, Hagerstown, MD) on top of a craniotomy over the left (monkey D) or the right (monkey T) parietal lobe (monkey D: 6.5 mm posterior/13 mm lateral, tilted backwards by 12°; monkey T: 9.2 mm posterior/13.1 lateral, 6°). For monkey D, chamber positions were based on anatomical MRI scans. Surgeries were performed aseptically under isoflurane anesthesia using standard techniques. All procedures were approved by the animal ethics committee of the district government of Braunschweig, Lower Saxony, Germany.

Apparatus

Experiments were performed in a dimly lit cabin. Monkeys sat in a custom made primate chair at a distance of 57 cm from a computer monitor on which visual stimuli were presented. The monitor covered 48° × 30° of visual angle at a resolution of 40 pixel/deg. Refresh rate was 75 Hz. Monkeys started a trial by touching a lever and responded by releasing the lever. Stimulus presentation, reward giving, and collection of behavioral as well as electrophysiological data was controlled by custom software developed in-house and run on an Apple Macintosh computer.

Electrophysiological Recordings

We recorded from 102 cells. Single unit action potentials were recorded extracellularly with either a single tungsten electrode (FHC, Inc., Bowdoinham, ME) or a 5 channel system (Mini Matrix, Thomas Recording, Giessen, Germany). The dura mater was penetrated with sharp guide tubes so that electrodes could be inserted into the brain by a hydraulic micropositioner (single electrode; David Kopf Instruments, Tujunga, CA) or a rubber tube drive (5 channel system). Impedances ranged from 1 to 8 MΩ.

Action potentials were recorded and sorted online using the Plexon data acquisition system (Plexon Inc., Dallas, TX). Data were filtered (frequency range 150–5 kHz) and amplified (gain range 1000–32 000), single unit waveforms were isolated by window discrimination.

Area MT was identified by its anatomical position, the high proportion of direction selective cells, and the typical size-eccentricity relationship of receptive fields (mean eccentricity 8.3° ± 0.3° SEM; mean diameter 9° ± 0.3° SEM (measured in the fixation condition, see below); mean direction selectivity index $(response_{preferred} - response_{antipreferred})/(response_{preferred} + response_{antipreferred})$ = 0.9 ± 0.02 SEM for the 81 cells for which tuning data were available offline).

Eye positions were monitored using a video-based eye tracking system (ET-49, Thomas Recording). Eye positions were recorded at 230 Hz, digitized and stored at 200 Hz. Fixation was controlled during the recordings to stay within a window of 1° radius around the fixation point (see below for details).

Experimental Procedure

After isolating a single unit, its cRF was identified by its response to a stationary random dot pattern (RDP) that was manually swept across the screen. To characterize speed and direction selectivity of the cell, the monkeys performed a task at the fixation point (0.3° × 0.3°, white, luminance contrast: 64.6% of full contrast at a background luminance of 0.02 cd/m^2), whereas a moving RDP (full contrast) was presented at the center of the estimated cRF. The task was the detection of a luminance change of the fixation point (luminance contrast after change: 53.4%). The size of the RDP was matched to the cRF size. Individual dot size was 0.1° × 0.1° at a dot density of 10 dots/deg^2. Motion speeds and directions were randomly drawn in intervals of 827 ms from 8 speeds logarithmically spaced between 0.5 and 64 deg/s and 12 evenly spaced directions between 0 (=upwards) and 330°. Responses to the individual speed–direction combinations were defined as mean firing rates in an interval of 80–800 ms after onset of the specific combination, and direction tuning curves were fit online with a circular Gaussian at each speed level. For the following experiments, a speed level was chosen at which there was a clear direction tuning, the direction yielding the highest response was defined as preferred direction and the opposite direction (180° apart) as antipreferred. When recording several units on different channels, we used a direction and speed combination that activated all units as strongly as possible.

Before the main experiment was started, we mapped the receptive field by presenting a brief RDP (the probe, full contrast, 187-ms presentations separated by 27 ms) moving in the preferred direction at several positions across the estimated receptive field. While the monkey performed a fixation task (detection of a luminance contrast change of the fixation point from 64.6% to 43.7%), the probe was presented in a random sequence at ~80 positions on a rectangular grid (probe grid) centered on the estimated cRF. The size of the probe and the probe grid as well as the number of probe positions was adjusted to each cell. The probe grid spanned a circular or elliptical region with a radius ~3 times the estimated cRF radius. Individual dots of the probe were 0.1° × 0.1° wide at a density of 8 dots/deg^2. We monitored online if the peak response was approximately in the middle of the probe grid. If it was, the main experiment was started using the same probe grid, otherwise, the probe grid was adjusted and the process was repeated.

Attention Task

For the main experiment, the monkeys were trained to attend to 1 of 2 moving RDPs (target and distractor) placed at equal eccentricity inside or near the estimated cRF borders. The trial started when the monkey fixated a yellow fixation spot (0.25° × 0.25°, luminance contrast: 92.7%) and held the lever. A stationary RDP (the cue) was presented for 440 ms at the later target location. After a delay of 133 ms, target and distractor appeared (luminance contrast: 46.5%), moving in the antipreferred direction. The antipreferred direction was used to keep baseline-firing rates and adaptation low, maximizing the influence of the probe. Ensuring that the stimulus was visible to the monkey and required that he performed a motion task precluded the use of a low-contrast and/or stationary stimulus. After another delay of 173 ms, a sequence of probe presentations started. The probe, a full contrast RDP moving in the preferred direction, was presented in random order at ~80 positions on the same probe grid used for the initial mapping, the positions which overlapped target and distractor

positions were skipped. Probes were presented for 187 ms, separated by 27 ms. Both target and distractor could change their direction of motion briefly (133 ms) by an angle of ~35°. Times of the direction changes were drawn independently for each stimulus from a flat distribution between 253 and 6000 ms after stimulus onset. The monkeys were rewarded immediately after they responded by lever release to the direction change of the target within a response time window of 150–650 ms after the direction change onset. If they reacted to the distractor change, did not respond within the response time window or broke fixation, the trial was aborted without reward. The baseline-firing rate of the neuron in each attentional condition was measured by skipping a probe in the sequence, that is within a 187-ms period the target and distractor stimuli were present without the probe, and this period was randomly interleaved with the probe presentations and had the same presentation statistics. This way we kept the influence of target and distractor stimuli constant across the measurement of probe responses and baseline. Figure 1 shows the trial sequence and stimulus arrangement.

As a control, we mapped the receptive field, while the monkeys performed the fixation task. After the monkeys started the trial, the fixation spot turned white (luminance contrast: 64.6%). There was no cue presentation; 2 RDPs (both distractors) appeared 553 ms after trial start at the same locations as target and distractor in the attention task. Otherwise the trial timing followed the same schedule as in the attention task. The monkeys were rewarded for the detection of a change of the fixation point from white to light gray (luminance contrast: 43.7%) between 253 and 6000 ms after stimulus onset. The changes of motion direction in the distractors had to be ignored. Note that sensory stimulation in and around the cRF did not differ between both attentional conditions as well as between attention and fixation conditions, so that all differences in neuronal responses and receptive field profiles are due to shifts in spatial attention.

Data Analysis

All calculations were performed with custom scripts written in MATLAB (The MathWorks, Natick, MA); all statistical tests were done using either MATLAB (The MathWorks) or SPSS (SPSS, Inc., Chicago, IL). Unless specified otherwise, errors given throughout the results are standard errors of the mean, statistical tests between unrelated groups are Mann–Whitney *U* tests, comparisons of related groups or tests of one sample are Wilcoxon signed rank tests, and correlations are Spearman rank correlations. We relied on nonparametric tests because some of the tested parameters did not seem to be normally distributed and contained outliers; and when comparing 2 unrelated groups of cells, in some cases the assumption of equal variances was not met. All significant results reported here were also significant using parametric procedures.

Receptive Field Maps

We analyzed neuronal data from hit trials only to ensure that attention was appropriately allocated to the cued location. We created receptive field maps for each task condition (2 attentional conditions and 1 fixation condition) from the mean firing rates 60–140 ms after probe onsets at each probe position. This time window was chosen to capture the strongest part of the excitatory/inhibitory response. Responses to probe positions which had been presented less than twice were excluded (mean probe presentation frequency across all positions, cells, and conditions was 20.71, median 20, lower quartile 15, and upper quartile 26, at a range of 2–62 presentations). From each mean firing rate we subtracted the mean baseline-firing rate measured in the respective task condition. Receptive field maps were computed by interpolating these response rates at each probe location with a cubic spline function. Interpolated maps were necessary to obtain continuous outlines for defining excitatory and inhibitory receptive field regions. Spline interpolation was chosen to keep the interpolation error low and to avoid strong assumptions about the shape of receptive field profiles.

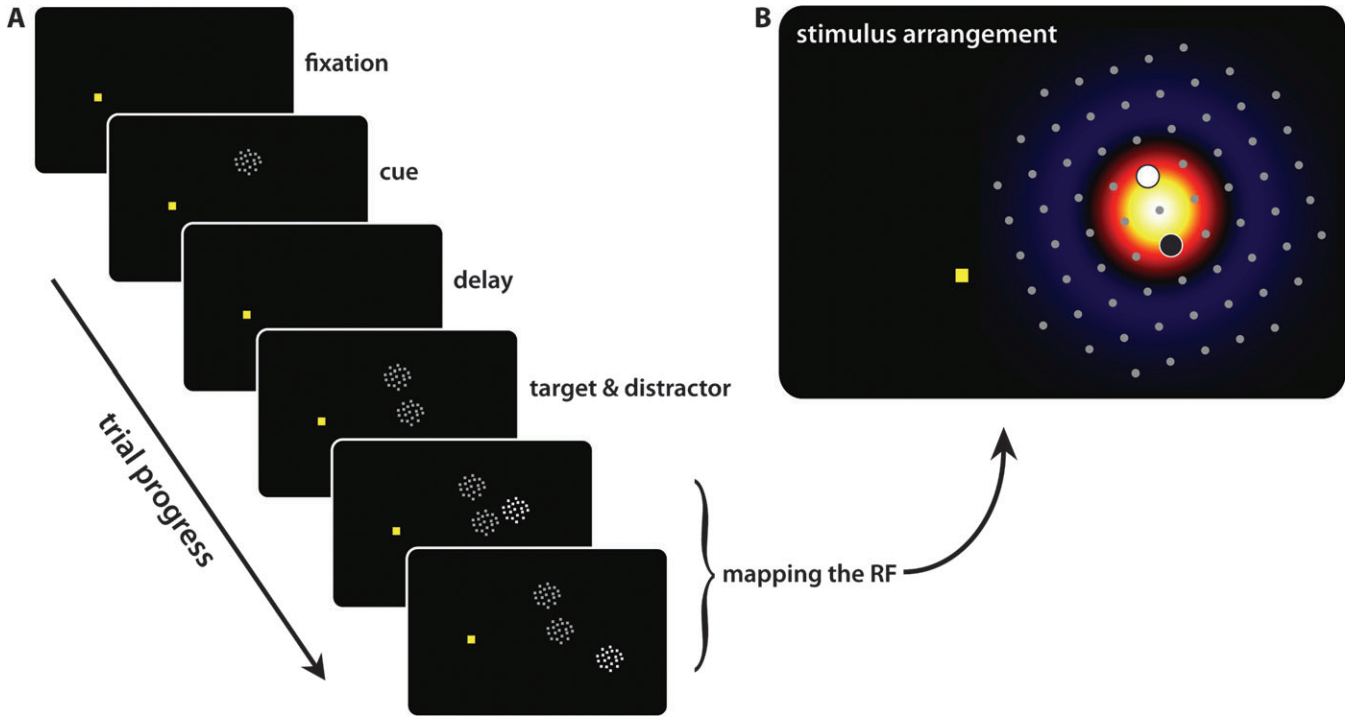

Figure 1. Attention task and stimulus arrangement. (*A*) The trial started with fixation of the yellow fixation point. A stationary RDP, shown for 440 ms, cued the later target position. After a delay of 133 ms, target and distractor RDPs appeared, moving in the antipreferred direction. After another 173 ms, the mapping of the receptive field with the probe started. The probe RDP, moving in the preferred direction, was presented in random order at ~80 positions for 187 ms each, separated by 27 ms. The monkey was rewarded for detecting a brief (133 ms) direction change of the target, which could occur between 253 and 6000 ms after target and distractor onset. (*B*) Target (black circle filled white) and distractor (white circle filled black) were presented in or next to the estimated receptive field center at equal eccentricity from the fixation point. The probe grid (light gray dots) spanned the receptive field center (red/yellow) and surround (blue) and was arranged so that either 1 or 2 probe positions fell onto the receptive field center, between the target and distractor RDPs. The illustration shows an ideal case were the full surround extent could be measured; often, the surround was larger than the mapped area. Drawings are not to scale.

The calculation of receptive field area and centroids are therefore based on the interpolated maps, whereas the definition of surround suppressed cells and the difference map analysis are based on the measured responses only (see below). For simplicity, we rotated all receptive field maps so that the fixation point was up, the target and distractor lay along the *x*-axis, and the midpoint between target and distractor was at the origin.

Identifying Excitatory and Inhibitory Receptive Field Regions

Based on the receptive field maps, we analyzed responses above and below baseline separately. For each, we defined a threshold of a quarter of the maximum excitatory/inhibitory modulation, a variant of the commonly used half-height approach (Lagae et al. 1994; Raiguel et al. 1995; Ben Hamed et al. 2002; Womelsdorf et al. 2006), to better accomodate the rather flat response modulation of the surround. Such a height-based criterion is analogous to defining the width of a spatial tuning curve at a particular height and has the advantage that it takes into account changes in receptive field amplitude. Patches of continuous points, which passed this threshold, were further constrained by including only patches which contained at least 2 sampled positions. Such a spatial coherence-based criterion removes spurious patches due to statistical fluctuations in individual probe responses and avoids an inappropriately large influence of very small patches in a potentially discontinuous center or surround surface. "Holes" within patches were treated in the same way. Two of the 102 cells were excluded from all further analysis because excitatory probe responses in the receptive field center were so weak that they did not pass this criterion.

Quantifying Inhibitory Surrounds

For each cell and each condition, we tested if the median of raw responses measured outside the excitatory center, which was defined as described above, was significantly below baseline in a 1-tailed sign test (alpha adjusted for multiple comparisons (100 cells × 3 conditions): 0.00017; overall significance level: 0.05). We classified a cell as having an inhibitory surround if the median firing rate outside the center was significantly below baseline in at least 1 of the 3 conditions, and only such "surround cells" were included in all analyses of surround modulations (58 cells).

Quantifying Shifts of Receptive Field Centers and Surrounds

Excitatory and inhibitory receptive field regions were analyzed separately. For each, we summed all height values from the interpolated maps falling into the patches which defined the respective receptive field region. The resulting value is a measure for the center and surround volumes. Note that because many surrounds appeared larger than the area we could measure, surround volume will refer only to the volume included in the region spanned by the probe grid. We calculated the centroid of this volume along the interstimulus axis as that *x*-value in the rotated map that divided the volume into halves. Even though the surround necessarily excluded the cRF, the surround centroid could nevertheless fall into this region. We then calculated shifts of center and surround volume centroids between the 2 attentional conditions, divided by the cRF diameter. Positive shift values indicate a shift toward the attentional focus, negative values a shift in the opposite direction. We tested if the mean shift values across cells were different from zero. We also correlated the shift magnitudes with the distance between the attention targets normalized to the cRF diameter.

Difference Map Analysis

Common models of receptive field center-surround structure assume a spatially overlapping center and surround (DeAngelis et al. 1994; Raiguel et al. 1995; Sceniak et al. 1999; Pack et al. 2005; Roberts et al. 2007). Within such a framework, center and surround measures are not independent of each other (Womelsdorf et al. 2008). To obtain a direct measure of the surround shift that is independent of the shift of the center, we analyzed systematic response change patterns within the inhibitory receptive field regions along the axis of the attentional targets (the "attentional shift" axis). To this end, "difference maps" were computed which plot the difference in response rate between the 2 attentional conditions for each probe position.

Difference maps were calculated for the 58 surround cells by first subtracting the response rates for each probe position when attention was on the left target in the rotated map from the corresponding response rates when attention was on the right target. For a pure center shift, the differences between response rates outside the center should scatter around zero, independent of the specific center-surround configuration. If there is a true surround shift, however, it would be visible as a systematic bias of response differences within the inhibitory receptive field regions left and right of the attentional targets: If the surround shifts with attention, this would yield difference values in the surround to be more positive on the left than on the right of the cRF (see Results and Supplementary Materials for details). Figure 4 and Supplementary Figure 3 show theoretical examples for different center-surround configurations. The figures also illustrate that the changes of response differences correlated to a surround shift are restricted to specific regions besides the cRF, depending on the symmetric/asymmetric arrangement of inhibitory regions around the cRF: Although a circularly symmetric surround as well as a surround that is asymmetric along the attentional shift axis would affect response differences besides the cRF along this axis, surrounds that are strongly asymmetric along the orthogonal axis would affect regions that are displaced from the center along the orthogonal. We therefore restricted our analysis to relevant parts of the difference maps, treating surrounds that were strongly asymmetric along the orthogonal to the attentional shift axis as a special case.

We identified the relevant regions of the difference map as follows: we first excluded all values belonging to the cRF in either of the 2 conditions. For defining both cRFs, we used the same procedure as described above but placed the threshold at 5% of the maximum excitatory modulation because the modulation of the cRF seemed to extend over a larger area than the cRFs themselves as they were originally defined. We found 2 cells with a surround asymmetry beyond that expected by chance. We used a conservative significance level (rank sum test of the median probe response in the fixation condition in the upper versus lower half outside the center, alpha 0.001), equivalent to an adjustment for multiple comparisons based on 58 cells, to treat only surrounds with a very strong asymmetry as an exception; using a significance level of 0.05 would classify 6 cells as having asymmetric surrounds.

Then, for the cells with surrounds that were not significantly asymmetric along the orthogonal axis, we limited the analyzed region at the top and bottom of the region corresponding to the 2 centers. For the 2 surrounds that were significantly asymmetric along this axis, we analyzed instead the (upper or lower) half exhibiting the stronger inhibition. For all cells, we computed the average of the response rate differences left and right of the origin of the map from the data points within the respective selected region. We then tested across cells if the average response rate difference on the left was different from the average response rate difference on the right. Supplementary Figure 2 illustrates the different steps of the difference map analysis. For visualization, the difference maps were interpolated using the same surface fit as for the original maps.

Receptive Field Area

We defined the square root of the area of the excitatory receptive field regions as the receptive field diameter. In the few cases in which the cRF consisted of several patches, we used the sum of their areas for calculating the diameter. Because by visual inspection of the maps we observed that many of our surrounds seemed to extend beyond the region covered by the probe grid, we do not provide a quantitative analysis of surround areas here. In order to investigate how attention modulates cRF size, we computed for each cell the relative size change in each of the attentional conditions with respect to the fixation condition ($\text{Diameter}_{\text{attention}} - \text{Diameter}_{\text{fixation}})/\text{Diameter}_{\text{fixation}}$; 2 size change values for each cell). Negative values indicate a shrinkage with attention, positive values an expansion. We divided the 200 attention–fixation pairs into those for which attention was directed *into* the cRF patch (142 cases) and those for which attention was directed to a location *next to* the cRF (=outside the quarter-height threshold; 58

cases). We tested if each group mean was significantly different from zero size change and if the group means were significantly different from each other, and we also determined the correlation between the size change and the distance of the attentional target from the cRF area centroid, normalized to the receptive field radius. We also tested if size changes were different for surround and nonsurround cells.

Analysis of Baseline, Peak Response, and Inhibition Strength

We compared the baseline-firing rate and the amplitude of the receptive field (=the maximum response after baseline subtraction) for all 100 cells in both attentional conditions with the same measures in the fixation condition. For the 58 surround cells, we also compared the absolute minimum firing rate outside of the cRF and the depth of the surround (=the minimum response after baseline subtraction) between the attention and fixation conditions. To find out if attentional modulation of any of these parameters was related to the exact location of the attentional focus inside or next to the cRF, we calculated the same tests after dividing the attention–fixation pairs into cases where the attentional target was inside the cRF and cases where attention was next to the cRF, and we calculated correlations between each of these parameters and the distance of the attentional target from the cRF center. We also directly compared the parameters between the 2 groups.

Because baseline changes, receptive field size changes, and the distance between receptive field center and attentional focus might be all inter-related, we were interested if the correlation between size change and distance was influenced by a correlation of the baseline change with this distance. Therefore, we calculated a partial correlation between size change and distance, controlling for the effect of the baseline change. Because the partial correlation relies on the parametric (Pearson) correlation, we removed outliers: we iteratively excluded cases which deviated from the mean by more than 4 standard deviations with respect to either baseline change, size change, or distance, until no cases remained which deviated by more than 4 standard deviations. By this procedure, 6 cases were excluded.

Eye Position Analysis

All analyses of receptive field parameters were done over periods in which the monkey maintained fixation within the 1° circular fixation window. Still, systematic differences of the eye position within the fixation window could cause a corresponding shift of retinotopic receptive fields. We analyzed eye positions over the same time periods from which the neuronal data were taken. We rotated eye positions so that they were aligned with the rotated receptive field maps, and then tested the difference in mean eye position projected onto the interstimulus axis, and the difference in mean eye position along the orthogonal axis along the center of the stimulus grid and the fixation

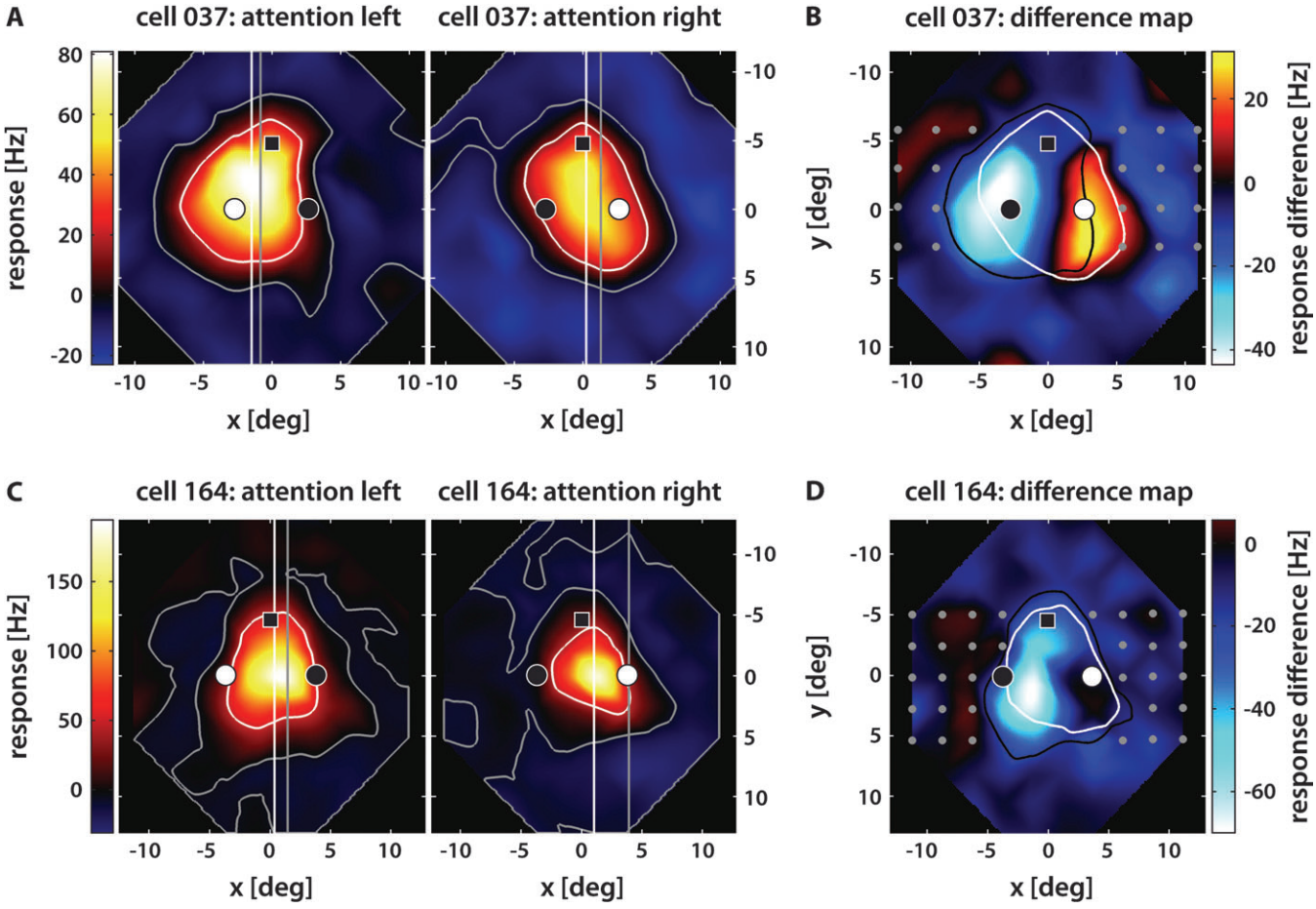

Figure 2. Center and surround shift for 2 example cells. (*A*, *C*) Receptive field maps for 2 example cells when attention was either on the left or on the right target (black circle filled white). Maps were rotated for convenience so that the fixation point (white square filled black) was up. The contour lines mark the quarter-height level of excitatory/inhibitory modulation at which center and surround were cut for the centroid analysis (white: center, gray: surround). The vertical lines show the volume centroids (white: center, gray: surround) along the target–distractor axis, calculated over the outlined area. For both cells, center and surround profiles shift toward the attended stimulus. (*B*, *D*) Difference maps for the same 2 cells were created by subtracting the probe responses with attention left from those with attention right. Regions of positive response differences (i.e., stronger response with attention right) are shown in red/yellow, whereas negative response differences are shown in blue/cyan. Contour lines mark the 5% level of the cRF for attention left (black contour) and attention right (white contour). The gray dots show the probe positions that were used to calculate the mean response differences left and right of both centers (see Methods for details). For both cells, the response differences are more positive on the left than on the right of the cRF, meaning that surround inhibition is weaker on the unattended side and stronger on the attended side.

point, between the 3 task conditions by using a 1-way repeated measures ANOVA (1 × 3 task conditions) and pairwise tests on the estimated marginal means. By this procedure, we analyzed eye positions along the same dimensions along which we analyzed receptive field shifts.

Behavioral Performance

As a measure of the monkeys' performance, mean hit rates and mean reaction times were averaged across cells. We compared performance between the attention and fixation conditions. These data are described in the supplementary materials (Supplementary Fig. 5).

Results

Our study is based on 100 single neurons recorded in area MT of 2 macaque monkeys (58 cells from monkey D and 42 cells from monkey T), whereas they directed their attention to one or the other of 2 stimuli placed within or next to the cRF of the neuron. For each neuron, we determined shifts of the excitatory receptive field center and of the inhibitory surround as well as changes of receptive field size, baseline-firing rates, peak responses, and inhibition strength with attention.

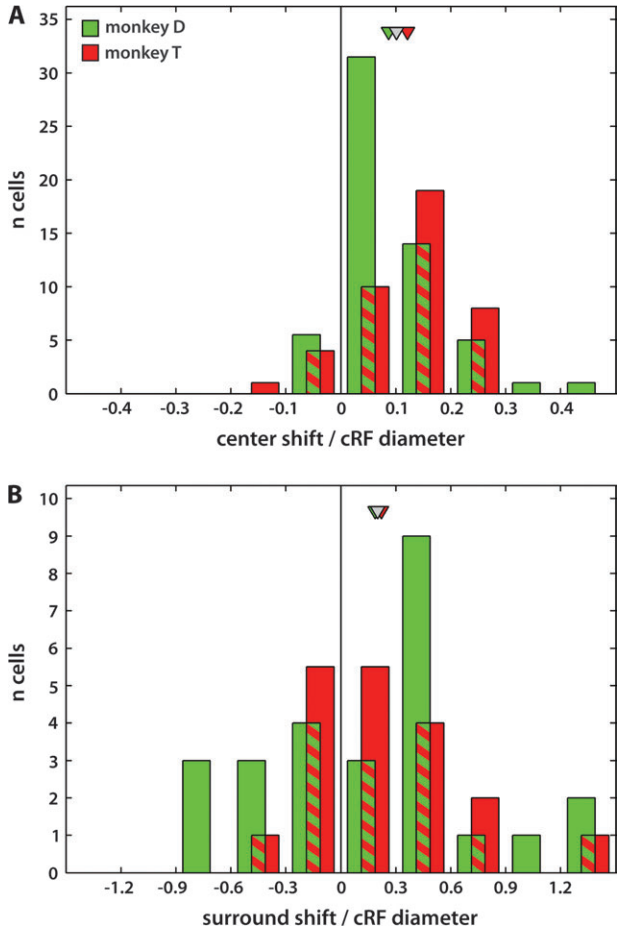

Figure 3. Distribution of center and surround shifts relative to the cRF diameter. (*A*) The histogram shows a significant shift of the cRF center toward the attended stimulus by 10.1% (±1% SEM, $P < 0.0005$, $n = 100$) of the cRF diameter (monkey D [green]: 8.7%, ± 1.2%, $P < 0.0005$, $n = 58$; monkey T [red]: 12.1%, ± 1.5%, $P < 0.0005$, $n = 42$). (*B*) The histogram shows a significant shift of the surround toward the attended stimulus by 20.2% (±7.7% SEM, $P = 0.022$, $n = 45$ cells in the surround centroid analysis) of the cRF diameter (monkey D: not significant, $P = 0.182$, $n = 26$; monkey T: 22.3%, ± 9.4%, $P = 0.043$, $n = 19$). Triangles mark the mean shift magnitudes (gray: overall, green: monkey D, red: monkey T).

Shifts of Receptive Field Center and Surround

The receptive fields were mapped under 2 attentional conditions: attention was either on the left stimulus or on the right stimulus, whereas the sensory stimulation and mapping procedure were exactly the same. Figure 2 shows 2 example cells. Indicated in the maps are the outlines of the excitatory (white) and inhibitory (gray) receptive field regions over which volume centroids for center and surround were determined. Center and surround shifts were defined as the difference in position of the respective centroid (white/gray vertical line) between the 2 attentional conditions, normalized to the cRF diameter. Both cells show a shift of the center as well as the surround toward the attended stimulus.

Figure 3*A* shows the distribution of normalized center shifts: On average, the receptive field center shifts by 10.1% (±1%) of its diameter toward the attended stimulus. This shift is highly significant ($P < 0.0005$) across cells. The average absolute magnitude of the center shift is 0.9° (±0.1°); and the average center shift normalized to the distance between the targets (the "attentional shift," i.e., the shift of spatial attention between the conditions) is 13.8% (±1.2%).

The shift of the inhibitory surround was analyzed for the surround cells ($n = 58$, see methods section for classification criteria). For some cells, surround strength strongly varied under different conditions. Thirteen cells completely lost their inhibitory surround in 1 of the conditions even when inhibition was strong in the other condition. In Figure 3*B*, the distribution of normalized surround shift values is plotted for the remaining 45 cells for which an inhibitory surround is present in both attentional conditions. They show a significant shift of the surround toward the attentional target, which is on average 20.2% (±7.7%) of the cRF diameter ($P = 0.022$). The average absolute magnitude of the surround shift is 1.6° (±0.7°); the average surround shift normalized to the attentional shift is 23.7% (±11.1%). Because some models of attentional cRF shifts predict a correlation of the shift magnitude with the distance of the attentional focus from the cRF center (Compte and Wang 2006), we analyzed if the receptive field shifts in our population were related to the spacing of the targets (which corresponds to twice the distance of the cRF center from the attentional focus), but we did not find such a correlation either for the center or surround when shift and target spacing were normalized to the receptive field size ($P = 0.604$ and $P = 0.169$ for center and surround, respectively).

To ensure that the surround shift described above is not just a consequence of the cell selection procedure employed, we repeated the analysis based on a less rigorous selection criterion. We selected those 74 cells for which any inhibitory patches reached threshold in both conditions, including cells which were not classified as surround cells. Based on this selection, the surround shift was only slightly reduced (14% ± 6.8% of the cRF diameter) and still significant ($P = 0.031$).

Dependence of Center and Surround Measurements

Typical receptive field center-surround structure can be well approximated by the difference of a peaked excitatory and a flatter inhibitory Gaussian, so that center and surround are spatially overlapping (DeAngelis et al. 1994; Raiguel et al. 1995; Sceniak et al. 1999; Pack et al. 2005; Roberts et al. 2007). Assuming such a model, the above shift measures for center and surround are not independent of each other (Womelsdorf et al.

2008). Specifically, the shift of the center might induce an apparent shift of the surround by covering or uncovering some of the inhibitory regions. This apparent shift could be in the opposite or in the same direction, depending on the exact alignment or asymmetry between center and surround and would be indicative of a change of inhibitory regions in the "effective" receptive field, but would not necessarily result from a change in those neuronal inputs that build the inhibitory surround. An apparent surround shift *opposite* to the center shift could have compensated a surround shift with attention, but we do observe a net shift *toward* the attentional focus. It is therefore important to clarify if the observed surround shift is a "true" surround shift or a side effect of the center shift. To obtain a direct measure of the surround shift that is independent of the shift of the center, we created difference maps by subtracting the probe responses of the 2 attentional conditions. If the center shifts but the surround itself does not, the differences between response rates outside the center should scatter around zero for all center-surround configurations. If there is a true surround shift, however, the map of response rate differences between the 2 attentional conditions should exhibit systematic changes. Figure 4 shows a hypothetical difference map for a cRF shift without surround shift (*A*) and with surround shift (*B*). Assuming no difference in overall response rate (amplitude) between the 2 attentional conditions, the cRF shift appears as a peak close to the target of the first condition and a dip near the target of the subtracted condition. For a shift of a circularly symmetric surround as in (*B*), there will be a bump of opposite sign at each side of the central bumps along the shift axis. If there is surround asymmetry along this axis, 1 of the bumps will be more pronounced than the other, whereas surround asymmetry along the orthogonal axis would shift the bumps along the *y*-axis, and a difference in overall response rates would shift the whole map away from zero. Nevertheless, in all cases the difference between the respective regions in the map left and right of the cRF would remain qualitatively the same. Figure 4 assumes a symmetric surround and no amplitude modulation with attention; in the supplementary materials we provide simulations of other configurations (Supplementary Fig. 3).

Figure 2*B* and *D* shows the difference maps for the 2 example neurons. "Attention left" has been subtracted from "attention right"; the cRF outlines and attention targets of both conditions are marked in black and white, respectively. For both cells, the shift of the center is clearly visible from the 2 bumps overlapping these regions. In cell 164 (*D*), there is an additional scaling of the receptive field between both conditions with responses being higher with "attention left," therefore all difference values are below zero. For both cells, the difference map is more positive on the left than on the right of the central region, consistent with a true shift of the inhibitory surround. Figure 5 shows the distribution of differences in means left and right across the same 58 surround cells that were included in the volume shift analysis: The average difference is 0.6 Hz (±0.2 Hz) and is significant across cells ($P = 0.013$).

In principle, the center shift could also be a side effect of the surround shift. We tested the group of 42 nonsurround cells and found the cRF shift within this group to be highly significant (mean 10.1% ± 1.2% of the cRF diameter, $P < 0.0005$, data not shown), so the shift of the center is not contingent on the shift of the surround. As another test for a dependency of center and surround shifts we compared the shift magnitudes for center

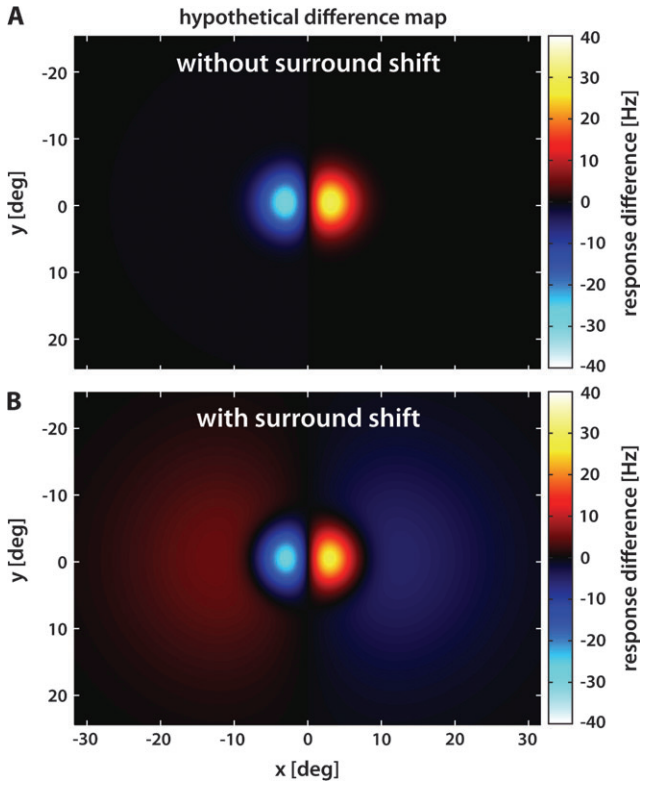

Figure 4. Hypothetical difference map. Hypothetical difference maps were created by subtracting 2 receptive field maps, each simulated by the difference of a narrow and peaked 2D-Gaussian (the receptive field center) and a spatially overlapping broad and flat 2D-Gaussian (the receptive field surround). (*A*) Only the cRF is shifted between both conditions. Here, a leftward shift of the receptive field center was subtracted from a rightward shift, resulting in a peak of positive response differences on the right and a dip of negative response differences on the left. (*B*) Attention additionally shifts the surround, resulting in an additional peak of positive response differences on the left and an additional dip of negative response differences on the right along the shift axis. See supplementary materials for further examples, formulas and choice of parameters.

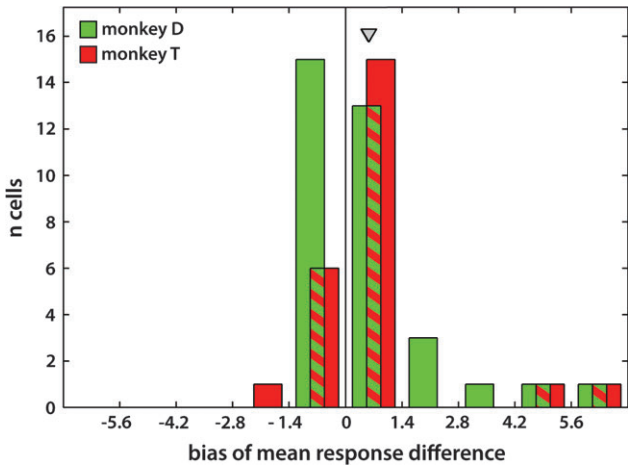

Figure 5. Distribution of the bias in mean response difference in the difference map analysis. The histogram shows a significant bias in mean response difference left and right of the cRF, so that the mean response difference is more positive on the left than on the right (mean 0.6 Hz ± 0.2 Hz SEM, gray triangle, $P = 0.013$, $n = 58$ surround cells), corresponding to weaker surround inhibition on the unattended side and stronger surround inhibition on the attended side. Both monkeys analyzed separately show the same trend (monkey D [green]: mean 0.6 Hz ± 0.3 Hz, $P = 0.092$, $n = 34$; monkey T [red]: mean 0.6 Hz ± 0.3 Hz, $P = 0.067$, $n = 24$).

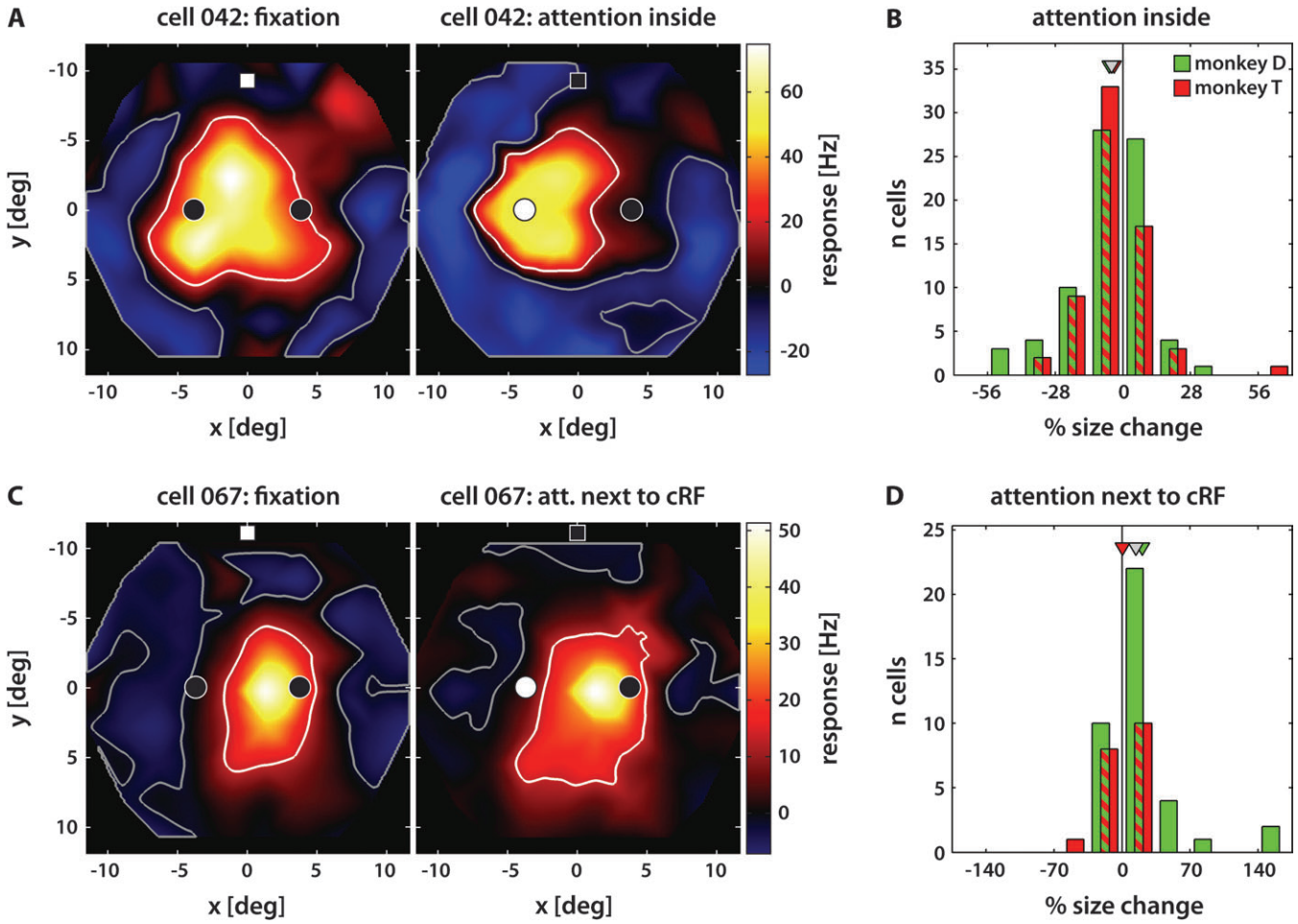

Figure 6. Size changes of the receptive field center with attention. (*A*) Receptive field maps of an example cell when a task was done at the fixation point (left graph, white filled square) and when a position inside the cRF was attended (right graph, black circle filled white). The cRF area, outlined in white, is clearly reduced with attention inside the cRF. (*B*) Plots the distribution of cRF size changes (in % of the cRF diameter in the fixation condition) for all 142 cases in which attention was directed into the cRF. There is a significant shrinkage of 4.7% (±1.3% SEM, $P < 0.0005$; monkey D: 5.6%, ± 1.8%, $P = 0.011$, $n = 77$; monkey T: 3.6%, ±1.7%, $P = 0.002$, $n = 65$). (*C*) Receptive field maps of another example cell are compared for the fixation task (left graph) and attending to a spot next to the cRF (outside of the quarter-height defined excitatory region; right graph). Here, the cRF area grows with attention. (*D*) Plots the distribution of cRF size changes for all 58 cases in which attention was directed to the border of the cRF. There is a significant expansion of 14.2% (±4.6% SEM, $P = 0.002$; monkey D: 20.8%, ±6.4%, $P < 0.0005$, $n = 39$; monkey T: not significant, $P = 0.717$, $n = 19$).

and surround and found no indication of such a relation (see supplementary materials for details).

cRF Size Changes

In a previous study on attentional modulation of receptive fields (Womelsdorf et al. 2006), we tested the hypothesis that receptive fields contract around an attended stimulus and found a small but significant shrinkage with attention. Here, we measured receptive field sizes across a wider range of target position distances. Figure 6 shows receptive fields of 2 single cells in the fixation condition and when attention was directed *into* the cRF (*A*) or allocated to a spot *next to* the cRF (*C*). Although the shrinkage of the cRF is clearly visible when attention is switched into the cRF, attention next to the cRF seems to expand rather than shrink the cRF. We found that across cells, the effects of attention on cRF size are different depending on the exact location of attention. Each cell contributes 2 values to this analysis because each attentional condition is independently compared with the fixation condition, so that sample size is 200 cases. For the group of 142 cases for which attention was switched into the cRF there is a highly significant mean shrinkage of cRF diameter by 4.7% (±1.3%, $P < 0.0005$). In contrast, for the group of 58 cases for which attention was directed to a location next to the cRF, there is a significant growth of the cRF diameter by 14.2% (±4.6%, $P = 0.002$). The average size change is also significantly different between the groups when directly compared with each other ($P < 0.0005$). Figure 6*B* and *D* plots the distributions of size changes for both groups. Figure 7 plots the size change of each attention–fixation pair as a function of the normalized distance between the attention target and the cRF area centroid: The change in cRF size correlates significantly with this distance ($r = 0.4$, $P < 0.0005$) and switches from shrinkage to expansion. In principle the change in cRF size could be an effect of the attentional modulation of the surround. To test for this possibility we analyzed the cRF size changes for the group of cells which lack surround suppression: We did not find any significant difference in cRF size modulation between surround cells and nonsurround cells ($P = 0.127$) and the difference in cRF size changes between cases with attention inside and besides the cRF is

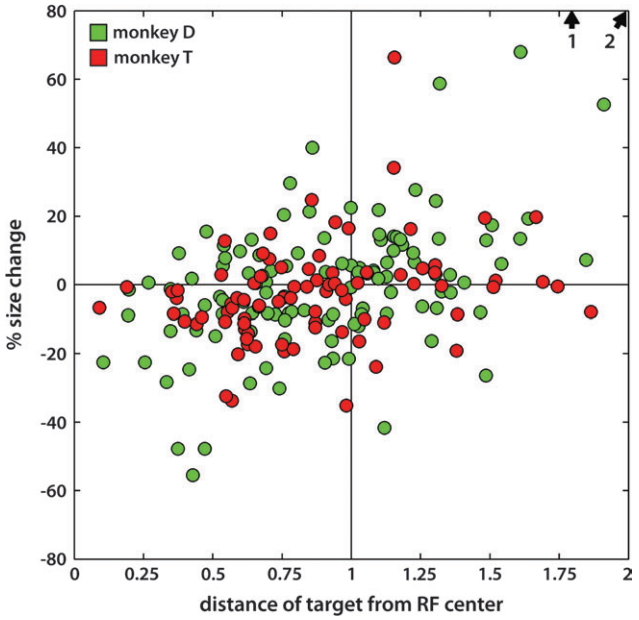

Figure 7. Receptive field size change as a function of the distance of the attentional target to the receptive field center. For the 200 attention–fixation pairs, the change in cRF diameter is plotted as a function of the distance between target and cRF center, which was normalized to the cRF radius so that a distance of 1 approximately marks the cutoff between attention inside and attention next to the cRF. Arrows mark data points that fall beyond the axis limits, numbers indicate how many data points are represented by each arrow. The correlation between size change and target-center distance is significant ($r = 0.4$, $P < 0.0005$; monkey D: $r = 0.46$, $P < 0.0005$, $n = 116$; monkey T: $r = 0.34$, $P = 0.002$, $n = 84$).

still significant if only nonsurround cells are analyzed (mean size changes: –4.1% ± 1.1%, $n = 66$, for attention inside and +2.6% ± 3.2%, $n = 18$, for attention besides the cRF; $P = 0.019$). Because these data show that the differential size change of the cRF occurs even in the absence of a surround, attentional modulation of the surround and effects on cRF size seem to result from independent mechanisms.

Baseline Shifts and Receptive Field Scaling

Because for some cells, baseline-firing rates, peak responses, and surround strength varied substantially between conditions, we determined if these variations were related to the allocation of attention into or near the cRF. We analyzed changes in baseline-firing rate, amplitude (the peak response relative to baseline), surround depth (the minimum response relative to baseline), and the minimum firing rate in the surround (without baseline subtraction).

Across all cells, the mean baseline-firing rate was 8.4 Hz in the fixation condition, and was significantly enhanced with attention by on average 1.5 Hz ± 0.4 Hz ($P = 0.006$). The baseline change is highly significant for those attention–fixation pairs for which the attentional focus was *inside* the cRF (2.3 Hz ± 0.6 Hz, $P < 0.0005$, $n = 142$), but not for those pairs with attention directed to a location *next to* the cRF ($P = 0.123$, $n = 58$). The difference in baseline change between the groups is highly significant ($P < 0.0005$), and we found a highly significant negative correlation of the baseline change with the distance of the attentional focus from the cRF center ($r = –0.33$, $P < 0.0005$).

Across cells, the mean cRF amplitude was 45.9 Hz in the fixation condition. Across all cells and also for the group of cases for which attention was oriented inside the cRF, there was no effect of attention on the amplitude (all: $P = 0.121$; "attention inside": $P = 0.981$), but for those cases for which attention was directed to the border of the cRF, we found a significant increase of cRF amplitude with attention (3.8 Hz ± 1.2 Hz, $P = 0.004$, $n = 58$). The difference in amplitude change between the groups is significant ($P = 0.014$), and we found a weak but significant correlation of the amplitude change with the distance of the attentional focus from the cRF center ($r = 0.163$; $P = 0.021$).

For the 58 surround cells, the mean surround depth was 5.8 Hz in the fixation condition. There was no overall effect of attention on the surround depth ($P = 0.937$). However, when attention was inside the cRF, surrounds tended to be deeper with attention (mean depth change 1 Hz ± 0.5 Hz, $P = 0.054$, $n = 76$); this effect just missed statistical significance. In contrast to this, when attention was allocated to a target near the cRF, surrounds became significantly shallower (1.4 Hz ± 0.7 Hz, $P = 0.004$, $n = 40$). This difference between the groups is highly significant ($P = 0.001$), and there is a correlation ($r = 0.35$, $P < 0.0005$) between the change in surround depth and the distance of the attentional focus from the cRF center.

Because surround depth was measured relative to baseline, a deepening or shallowing of surrounds does not necessarily result from a change of the strength of inhibitory responses, but might instead be a consequence of systematic baseline changes. Indeed, we found that the absolute minimum firing rate (without baseline subtraction) was *higher* in the attentional conditions than in the fixation condition (mean difference 0.8 Hz ± 0.3 Hz, $P < 0.0005$, at an average minimum rate of 1.8 Hz in the fixation condition). This increase is significant for those attention–fixation pairs for which the attentional focus was *inside* the cRF as well as for those cases with attention *next to* the cRF (attention inside: 1 Hz ± 0.4 Hz, $P < 0.0005$, $n = 76$; attention near: 0.5 Hz ± 0.1 Hz, $P = 0.001$, $n = 40$; the difference between the groups is not significant although there is a trend, $P = 0.091$), so that the change in relative surround depth must be related to the change in baseline-firing rate.

We performed several analyses to control if these effects on baseline-firing rate could have influenced our measurement of receptive field sizes and shifts: Firstly, because receptive field sizes were determined from baseline-corrected maps, we were wondering if the differential changes in baseline-firing rate depending on the location of the attentional target influenced our analysis of receptive field shrinkage and expansion. We indeed found a clear correlation between baseline change and size change (rank correlation $r = –0.61$, $P < 0.0005$, $n = 200$; Pearson correlation $r = –0.46$, $P < 0.0005$, $n = 194$ after outlier correction [see Methods]), but we also found a partial correlation between size change and distance of the attentional target from the cRF center, controlling for baseline changes ($r = 0.29$, $P < 0.0005$, $n = 194$ after outlier correction [see Methods]). This means that the variation of cRF size changes with distance from the attentional focus is related to the baseline changes, but is not completely explained by it. Secondly, if baseline changes were systematically different *between* attentional conditions, this might have influenced the measure of cRF and surround shifts. Although as mentioned above, for some cells the baseline, cRF amplitude and surround

depth seemed highly variable between the attentional conditions, across cells, the differences in baseline, amplitude, and depth were not significantly different from zero, so baseline changes could not influence our shift measures in any systematic way (baseline: $P = 0.365$; amplitude: $P = 0.864$; depth: $P = 0.306$).

Eye Positions

Systematic differences of the monkeys' eye position within the fixation window could in principle cause a corresponding shift of the mapped receptive fields. We tested for a shift in eye position along the interstimulus axis across cells using a 1-way repeated measures ANOVA (1 × 3 task conditions). There was no significant main effect on the eye position along the interstimulus axis ($P = 0.162$), but pairwise comparisons of estimated marginal means yielded a very small yet significant difference between eye position in the 2 attentional conditions (mean difference = 0.02°, $P = 0.014$). Such a small shift in eye position cannot account for the much larger shift of receptive field position. Furthermore, the eye position difference was in the opposite direction as the observed receptive field shift and therefore cannot contribute to it. In a further assessment of eye position effects, we did not find a significant correlation between eye position difference along this axis and either center or surround shifts between the attentional conditions (here, the absolute shift values were used; center: $P = 0.419$; surround: $P = 0.892$), and we also did not find a correlation between eye position difference and the result of the difference map analysis ($P = 0.241$). There was, however, a significant difference of the eye position along the orthogonal axis between the fixation task and both of the attentional conditions: eye positions were closer to the RDPs when the monkeys were involved in the attention task (main effect of condition: $P = 0.008$, pairwise comparisons of estimated marginal means between fixation and attention condition 1 and 2: mean = 0.03, $P = 0.078$ and mean = 0.03, $P = 0.013$). This should not influence any comparisons between the 2 attentional conditions, though. Supplementary Figure 4 shows the distribution of eye positions in the 3 task conditions for the example cells from Figure 2 and the distribution of mean eye positions across all cells.

Discussion

Switching spatial attention between 2 stimuli inside or near an MT neuron's cRF shifts the center of the cRF as well as the inhibitory surround profile toward the attended stimulus. Center shifts were on average 10.1% of the receptive field diameter, whereas the surround profile shifted by twice this distance, 20.2% of the cRF diameter. Systematic changes of surround strength on the attended and unattended side of the receptive field represent an attentional modulation of the surround itself, independent of the attentional effects on the cRF. Furthermore, cRF sizes are reduced when attention is directed *into* the receptive field by 4.7%, but expanded by 14.2% if the attentional target is *next to* the cRF. Absolute surround strength can be highly variable for the same cell when measured under different attentional conditions: surrounds tend to be deepened if attention is directed *into* the cRF but are significantly shallowed if the attentional target is *next to* the cRF. This is related to changes in baseline-firing rate, which is enhanced for attentional targets inside the cRF but not for attentional targets next to the cRF. Baseline modulation is correlated to receptive field size changes, but cannot explain the total variation of the shrinkage/expansion effect with distance from the attentional focus.

Because very often surround regions seemed to extend beyond the borders of the mapped area, in principle different shift results could have been obtained if the whole surround was measured. This seems unlikely though, given that typical models of surround suppression assume that suppression is strongest near/overlapping the cRF and decreases with distance from the cRF (DeAngelis et al. 1994; Raiguel et al. 1995; Sceniak et al. 1999; Pack et al. 2005; Roberts et al. 2007). Also, we measured the same critical part of the surround in both attentional conditions, so that missing parts of the surround should influence the receptive field map in both conditions in the same manner and should therefore not bias the shift measure. The spatially nonspecific up- and down-modulation of surround inhibition relative to baseline should not be affected by this restriction to measurement of the most central part of the surround.

By shifting excitatory and inhibitory regions toward an attended location, attention modulates the profile of a single neuron's spatial tuning function in a nonmultiplicative fashion. Because on average the shift of the surround is larger than that of the center, the effect is not just a position shift of the spatial tuning curve as a whole. Instead, excitatory gain and surround suppression both become stronger at/near the attended location, reshaping the spatial configuration of the receptive field complex.

Possible Mechanisms of a Surround Shift

Receptive fields are commonly thought to increase in size and complexity as one moves up the visual hierarchy by spatially pooling across more and more inputs from lower-level areas. Attention may differentially modulate the gain of lower-level receptive fields (e.g., in V1) representing the attended and unattended locations and thereby cause a biased weighting of inputs to receptive fields in higher-level areas like MT, which would lead to a shift of excitatory receptive field profiles in the higher-level area toward the attended position (Maunsell and McAdams 1999, 2001; McAdams and Maunsell 1999). Such a feedforward model has been shown to be able to account for cRF shifts toward the attentional focus given a relatively large spatial spread of attention (Compte and Wang 2006; Womelsdorf et al. 2008).

In contrast to excitatory receptive field regions, which are mainly built from feedforward connections, there are several possibilities how antagonistic surrounds could arise in area MT, which are not necessarily mutually exclusive. One possibility is that the center-surround structure of feedforward input is transferred to MT receptive fields (Tanaka et al. 1986). On the other hand, MT is reciprocally connected to areas MST and VIP (Maunsell and Van Essen 1983) and these higher visual areas with large receptive fields could create antagonistic surrounds in area MT via feedback connections (Tanaka et al. 1986), a hypothesis supported by the finding that response latencies are longer in the surround than in the center (Allman et al. 1985; Perge et al. 2005). Alternatively, surrounds could be created within area MT, either by horizontal connections (Allman et al. 1985), or by inhibitory connections from especially large

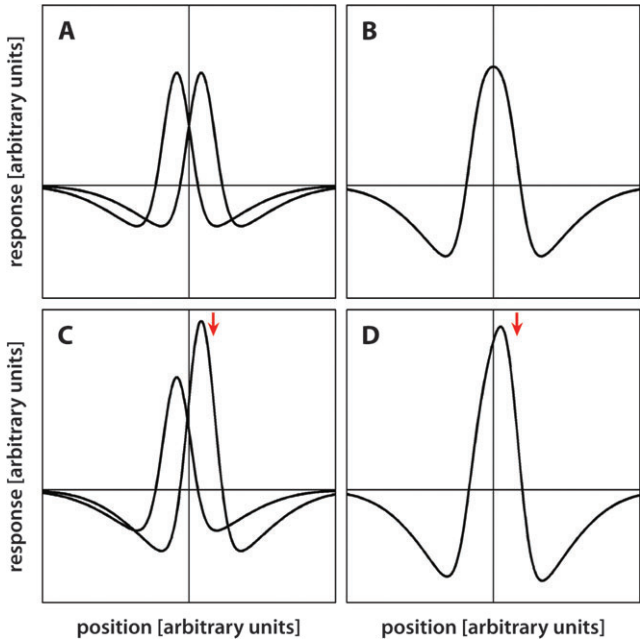

Figure 8. A mechanism for a feedforward surround shift. (*A*) Spatial tuning profiles (response as a function of position) of 2 V1 receptive fields with inhibitory surrounds are represented by the difference of 2 Gaussians. (*B*) Their additive combination results in a broader spatial tuning curve, with inhibitory surround, representing the receptive field of an MT neuron. (*C* and *D*) The same receptive fields are shown with attention selectively increasing the gain of that V1 receptive field closer to the attentional focus (marked by the red arrow): multiplicative gain modulation of one of the V1 receptive fields (*C*) shifts the peak of the MT receptive field toward the direction of spatial attention, and at the same time increases surround strength on the same side (*D*).

receptive fields found in layer 5 (Raiguel et al. 1995). Consistent with the latter view, the deeper layers (4–6) in area MT contain most of the cells without inhibitory surround (Tanaka et al. 1986; Raiguel et al. 1995; Lui et al. 2007).

Given our paradigm for mapping the inhibitory surround, it is possible that we stimulate mainly feedforward components of the surround. Our paradigm differs from earlier approaches in 2 respects: we do not present an optimal stimulus inside the cRF while mapping the surround, and we stimulate the surround using brief probes which might not be optimal for a full-blown surround suppression known to lag behind the excitatory response by between 16 ms (Perge et al. 2005) and 40 ms (Allman et al. 1985). Still, we find significant suppressive responses and systematic shifts of surround volume demonstrating that our method captures the surround. Although it is possible that such a paradigm underestimates overall surround strength, it does not bias the measurement of surround position, which is our main interest here. Because the influence of target and distractor was kept constant across all experimental conditions, an interaction of probe and target/distractor responses cannot explain any of the observed differences in center and surround position, size, or strength, between conditions.

Assuming that MT surrounds do have a strong feedforward component in which the center-surround structure of V1 receptive fields is contained, a similar mechanism could shift excitatory and inhibitory receptive field regions: Attentional gain modulation could selectively strengthen the surrounds of those V1 receptive fields which overlap the attended location and so deepen the surround of an MT neuron selectively on the attended side of its receptive field—this would shift the inhibitory surround profile in MT toward the attentional focus (Fig. 8). Recent research however suggests that such an attentional strengthening of surround inhibition in V1 occurs only for parafoveal receptive fields, whereas surround inhibition seems to be weakened by attention at eccentricities more similar to those sampled in our study (Roberts et al. 2007). To which extent characteristics of task and stimulus influence this finding needs further investigation: it is conceivable that at low contrast, which is known to enhance spatial summation rather than segmentation in V1 (Kapadia et al. 1999; Sceniak et al. 1999), attention strengthens summation even more, but at high contrast, which favors segmentation, attention might have the opposite effect.

Another mechanism is suggested by a recent study by Chen et al. (2008, see also comment by Reynolds 2008), who report that different cell types in area V1 are differentially affected by attention inside or outside their receptive field. Although narrow spiking neurons (putative inhibitory interneurons) tend to be enhanced by increased attentional load at their cRF, broad spiking neurons (putative pyramidal neurons) tend to be suppressed by increased attentional load outside their cRF. If these inhibitory interneurons are involved in creating the inhibitory surround of the pyramidal cells, then their enhancement could explain a spatially specific enhancement of surround suppression of pyramidal neurons near the attentional focus. The shift of surround inhibition toward the attentional focus we find in area MT could therefore be inherited from V1 pyramidal cells.

At least a component of MT surrounds may be formed by connections coming from larger receptive fields found either in higher visual areas or particular layers within area MT (see above). How those large receptive fields could provide the spatial specificity required to induce a surround shift is not clear.

Functional Implications of a Surround Shift

A large amount of research has established antagonistic surrounds as a general organizing principle throughout the visual system and current research discovers more and more of their complex spatiotemporal characteristics. Although antagonistic surrounds are associated with a variety of different perceptual functions, the direct link is not completely understood. Generally, center-surround organization has been implicated in figure-ground segregation (Lamme 1995; Zipser et al. 1996; Yazdanbakhsh and Livingstone 2006), pop-out (Kastner et al. 1997), the detection of line ends and curvature (Julesz 1981; Dobbins et al. 1987; Dobbins et al. 1989), and perceptual constancy (Allman et al. 1985). Motion sensitive surrounds in particular have been suggested to be important for image segmentation based on motion as well as perceiving relative motion of objects and self-motion in the environment (Allman et al. 1985; Bradley and Andersen 1998; Born et al. 2000). The asymmetric center-surround structures found in area MT may be useful for extracting shape from motion (Buracas and Albright 1996; Liu and Van Hulle 1998).

In the present experiment, the attentional targets were almost always in excitatory regions of the receptive field or between excitatory and inhibitory regions, but nearly never within the deep portions of the surround. Therefore, shifts

such as the one observed would typically bring the relevant stimulus into the cRF or closer to the cRF center, whereas the surround inhibition is strengthened just beyond the attended location. Such a shift might function to increase the attended stimulus' influence on the cell's response but also to actively suppress stimulation in its close vicinity and reduce influences of distractors, thus enhancing spatial resolution (Tzotsos et al. 1995; Cutzu and Tzotsos 2003). A strengthening of center-surround antagonism at the attended location would also improve the perception of local-to-local motion contrast.

In previous studies, facilitatory influences from the non-cRF have been reported in area MT: Some MT neurons have surrounds that act facilitatory when stimulated with the antipreferred direction (Allman et al. 1985; Tanaka et al. 1986) and thereby seem to contribute to the processing of differential object/background motion. Another class of MT neurons responds best to large fields of homogeneous motion, so that stimulation of the surround with the preferred direction acts facilitatory (Born and Tootell 1992; Born et al. 2000). Because we only used preferred direction stimuli as mapping probes we could not test for facilitation by antipreferred direction stimulation in the surround and could not differentiate between nonsurround cells and cells which react to wide-field motion. Therefore we do not know if attention modulates facilitatory influences from the non-cRF, but if such influences are indeed strengthened near the attentional focus, attention might emphasize differential processing of stimuli near the attentional focus by different cell types differing in their spatial integration properties.

Integrative and Suppressive Receptive Field Properties are Variable with Attention

Our observation of changes in surround strength in MT is reminiscent of reports of attentional effects on receptive field surrounds in V1: attention changes integrative and suppressive receptive field characteristics (Roberts et al. 2007); an effect that has also been found with variations in stimulus contrast (Kapadia et al. 1999; Sceniak et al. 1999). Together these findings challenge the concept of an inhibitory surround as a fixed property of a given neuron.

We found a trend of surround depth to vary systematically with the distance of the receptive field from the attentional focus, so that surrounds tended to be deep when attention was within the excitatory part of the receptive field but shallower with attention next to the receptive field. Additionally, we found systematic changes in the size of the excitatory receptive field center: when attention was allocated inside the cRF borders, the cRF contracted around the attended stimulus, but when attention was directed outside, the cRF grew toward the attended stimulus. Such a switch from cRF shrinkage to cRF expansion is predicted by the feedforward model of attentional modulation proposed by Compte and Wang (2006). Both, an increase in cRF size as well as a shallowing of surround inhibition would lead to spatial integration of sensory inputs over a wider area, whereas the shrinkage of the cRF together with a stronger surround inhibition would favor segmentation of the scene. An expansion of nearby receptive fields toward the focus of attention allocates more neuronal resources to the attended stimulus. On the other hand, receptive fields which already include the attended stimulus might receive stronger surround inhibition in order to suppress distractive signals from outside. In both cases the shift of the receptive field profile brings the attended stimulus closer to excitatory receptive field regions while suppressing nearby locations more strongly.

In summary, we provide evidence that attention optimizes MT receptive fields by shifting excitatory receptive field centers and inhibitory receptive field surrounds toward an attended stimulus. This nonmultiplicative push–pull modulation combines with adaptive cRF size changes and a general up- and downmodulation of integrative versus suppressive surround. This optimizes spatial selectivity for the representation of the attended stimulus at the expense of distractors.

Supplementary Material

Supplementary material can be found at: http://www.cercor.oxfordjournals.org/

Funding

International Max Planck Research School for Neurosciences, Göttingen; and the German Ministry for Education and Science Grant (BMBF 01GQ0433) to the Bernstein Center for Computational Neuroscience, Göttingen. Funding to pay the Open Access publication charges for this article was provided by the German Primate Center, Göttingen.

Notes

We thank D. Prüsse, L Burchardt, S. Plümer, and R. Brockhausen for excellent technical assistance, S. Stuber, and B. Glaser for administrative assistance, Dr T. Tzvetanov for productive discussions and comments about earlier versions of this manuscript and 2 anonymous reviewers for helpful comments. *Conflict of Interest*: None declared.

Address correspondence to Dr Katharina Anton-Erxleben, Cognitive Neuroscience Laboratory, German Primate Center, Kellnerweg 4, 37077 Göttingen, Germany. Email: kantonerxleben@dpz.gwdg.de.

References

Allman J, Miezin F, McGuiness E. 1985. Direction- and velocity-specific responses from beyond the classical receptive field in the middle temporal visual area (MT). Perception. 14:105–126.

Ben Hamed S, Duhamel J-R, Bremmer F, Graf W. 2002. Visual receptive field modulation in the lateral intraparietal area during attentive fixation and free gaze. Cereb Cortex. 12(3):234–245.

Bradley DC, Andersen RA. 1998. Center-surround antagonism based on disparity in primate area MT. J Neurosci. 18(18):7552–7565.

Brefczynski JA, DeYoe EA. 1999. A physiological correlate of the 'spotlight' of visual attention. Nat Neurosci. 2(4):370–374.

Born RT, Groh JM, Zhao R, Lukasewycz SJ. 2000. Segregation of object and background motion in visual area MT: effects of microstimulation on eye movements. Neuron. 26(3):725–734.

Born RT, Tootell RBH. 1992. Segregation of global and local motion processing in primate middle temporal visual area. Nature. 357:497–499.

Buracas GT, Albright TD. 1996. Contribution of area MT to perception of three-dimensional shape: a computational study. Vision Res. 36(6):869–887.

Carrasco M, Williams PE, Yeshurun Y. 2002. Covert attention increases spatial resolution with or without masks: support for signal enhancement. J Vision. 2:467–479.

Chen Y, Martinez-Conde S, Macknik SL, Bereshpolova Y, Swadlow HA, Alonso J-M. 2008. Task difficulty modulates the activity of specific neuronal populations in primary visual cortex. Nat Neurosci. 11(8):974–982.

Compte A, Wang X-J. 2006. Tuning curve shift by attention modulation in cortical neurons: a computational study. Cereb Cortex. 16:761–778.

Connor CE, Gallant JL, Preddie DC, Van Essen DC. 1996. Responses in area V4 depend on the spatial relationship between stimulus and attention. J Neurophysiol. 75(3):1306–1308.
Connor CE, Preddie DC, Gallant JL, Van Essen DC. 1997. Spatial attention effects in macaque area V4. J Neurosci. 17(9):3201–3214.
Cutzu F, Tzotsos JK. 2003. The selective tuning model of attention: psychophysical evidence for a suppressive annulus around an attended item. Vision Res. 43:205–219.
DeAngelis GC, Freeman RD, Ohzawa I. 1994. Length and width tuning of neurons in the cat's primary visual cortex. J Neurophysiol. 71(1):347–374.
Dobbins A, Zucker SW, Cynader MS. 1987. Endstopped neurons in the visual cortex as a substrate for calculating curvature. Nature. 329:438–441.
Dobbins A, Zucker SW, Cynader MS. 1989. Endstopping and curvature. Vision Res. 29(10):1371–1387.
Haenny PE, Schiller PH. 1988. State dependent activity in monkey visual cortex. I. Single cell activity in V1 and V4 on visual tasks. Exp Brain Res. 69(2):225–244.
Hawkins HL, Hillyard SA, Luck SJ, Mouloua M, Downing C, Woodward DP. 1990. Visual attention modulates signal detectability. J Exp Psychol Hum Percept Perform. 16(4):802–811.
Huang X, Albright TD, Stoner GR. 2007. Adaptive surround modulation in cortical area MT. Neuron. 53:761–770.
Ito M, Gilbert CD. 1999. Attention modulates contextual influences in the primary visual cortex of alert monkeys. Neuron. 22:593–604.
Julesz B. 1981. Textons, the elements of texture perception, and their interactions. Nature. 290:91–97.
Kapadia MK, Westheimer G, Gilbert CD. 1999. Dynamics of spatial summation in primary visual cortex of alert monkeys. Proc Natl Acad Sci USA. 96(21):12073–12078.
Kastner S, Nothdurft H-C, Pigarev IN. 1997. Neuronal correlates of pop-out in cat striate cortex. Vision Res. 37(4):371–376.
Lagae L, Maes H, Raiguel S, Xiao D-K, Orban GA. 1994. Responses of macaque STS neurons to optic flow components: a comparison of areas MT and MST. J Neurophysiol. 71(5):1597–1626.
Lamme VAF. 1995. The neurophysiology of figure-ground segregation in primary visual cortex. J Neurosci. 15(2):1605–1615.
Liu L, Van Hulle MM. 1998. Modeling the surround of MT cells and their selectivity for surface orientation in depth specified by motion. Neural Comput. 10:295–312.
Lui LL, Bourne JA, Rosa MGP. 2007. Spatial summation, end inhibition and side inhibition in the middle temporal visual area (MT). J Neurophysiol. 97:1135–1148.
Martinez-Trujillo JC, Treue S. 2004. Feature-based attention increases the selectivity of population responses in primate visual cortex. Curr Biol. 14:744–751.
McAdams C, Maunsell JHR. 1999. Effects of attention on orientation-tuning functions of single neurons in macaque cortical area V4. J Neurosci. 19(1):431–441.
Maunsell JHR, McAdams CJ. 1999. Effects of attention on neuronal response properties in visual cerebral cortex. In: Gazzaniga MS, editor. The new cognitive neurosciences. Cambridge (MA): MIT Press. p. 315–324.
Maunsell JHR, McAdams CJ. 2001. Effects of attention on the responsiveness and selectivity of individual neurons in visual cerebral cortex. In: Braun J, Koch C, Davis JL, editors. Visual attention and cortical circuits. Cambridge (MA): MIT Press. p. 103–119.
Maunsell JHR, Van Essen DC. 1983. The connections of the middle temporal visual area (MT) and their relationship to a cortical hierarchy in the macaque monkey. J Neurosci. 3(12):2563–2586.
O'Regan JK, Rensink RA, Clark JJ. 1999. Change-blindness as a result of 'mudsplashes'. Nature. 398:34.
Pack CC, Hunter JN, Born RT. 2005. Contrast dependence of suppressive influences in cortical area MT of alert macaque. J Neurophysiol. 93:1809–1815.
Perge JA, Borghuis BG, Bours RJE, Lankheet MJM, van Wezel RJA. 2005. Dynamics of directional selectivity in MT receptive field centre and surround. Eur J Neurosci. 22:2049–2058.
Posner MI, Snyder CR, Davidson BJ. 1980. Attention and the detection of signals. J Exp Psychol. 109(2):160–174.
Raiguel S, Van Hulle MM, Xiao D-K, Marcar VL, Orban GA. 1995. Shape and spatial distribution of receptive fields and antagonistic motion surrounds in the middle temporal area (V5) of the macaque. Eur J Neurosci. 7(10):2064–2083.
Reynolds JH. 2008. Mapping the microcircuitry of attention. Nat Neurosci. 11(8):861–862.
Reynolds JH, Pasternak T, Desimone R. 2000. Attention increases sensitivity of V4 neurons. Neuron. 26:703–714.
Roberts MJ, Delicato LS, Herrero J, Gieselmann MA, Thiele A. 2007. Attention alters spatial integration in macaque V1 in an eccentricity-dependent manner. Nat Neurosci. 10(11):1483–1491.
Sceniak MP, Ringach DL, Hawken MJ, Shapley R. 1999. Contrast's effect on spatial summation by macaque V1 neurons. Nat Neurosci. 2(8):733–739.
Serences JT, Yantis S. 2006. Selective visual attention and perceptual coherence. Trends Cogn Sci. 10(1):38–44.
Spitzer H, Desimone R, Moran J. 1988. Increased attention enhances both behavioral and neuronal performance. Science. 240(4850):338–340.
Tanaka K, Hikosaka K, Saito H, Yukie M, Fukada Y, Iwai E. 1986. Analysis of local and wide-field movements in the superior temporal visual areas of the macaque monkey. J Neurosci. 6(1):134–144.
Tootell RBH, Hadjikhani N, Hall EK, Marrett S, Vanduffel W, Vaughan JT, Dale AM. 1998. The retinotopy of visual spatial attention. Neuron. 21:1409–1422.
Treue S. 2003. Visual attention: the where, what, how and why of saliency. Curr Opin Neurobiol. 13:428–432.
Treue S, Martinez-Trujillo JC. 1999. Feature-based attention influences motion processing gain in macaque visual cortex. Nature. 399:575–579.
Treue S, Maunsell JHR. 1996. Attentional modulation of visual motion processing in cortical areas MT and MST. Nature. 382:539–541.
Treue S, Maunsell JHR. 1999. Effects of attention on the processing of motion in macaque middle temporal and medial superior temporal visual cortical areas. J Neurosci. 19(17):7591–7602.
Tzotsos JK, Culhane SM, Wai WYK, Lai Y, Davis N, Nuflo F. 1995. Modelling visual attention via selective tuning. Artificial Intelligence. 78:507–545.
Williford T, Maunsell JHR. 2004. Effects of spatial attention on contrast response functions in macaque area V4. J Neurophysiol. 96:40–54.
Womelsdorf T, Anton-Erxleben K, Pieper F, Treue S. 2006. Dynamic shifts of visual receptive fields in cortical area MT by spatial attention. Nat Neurosci. 9(9):1156–1160.
Womelsdorf T, Anton-Erxleben K, Treue S. 2008. Receptive field shift and shrinkage in macaque area MT through attentional gain modulation. J Neurosci. 28(36):8934–8944.
Xiao D-K, Raiguel S, Marcar V, Koenderink J, Orban GA. 1995. Spatial heterogeneity of inhibitory surrounds in the middle temporal visual area. Proc Natl Acad Sci USA. 92:11303–11306.
Yazdanbakhsh A, Livingstone MS. 2006. End stopping in V1 is sensitive to contrast. Nat Neurosci. 9(5):697–702.
Yeshurun Y, Carrasco M. 1998. Attention improves or impairs visual performance by enhancing spatial resolution. Nature. 396(6706):72–75.
Zipser K, Lamme VAF, Schiller PH. 1996. Contextual modulation in primary visual cortex. J Neurosci. 16(22):7376–7389.